A Buried Polar Interaction Can Direct the Relative Orientation of Helices in a Coiled Coil†

Martha G. Oakley‡ and Peter S. Kim*

Howard Hughes Medical Institute, Whitehead Institute for Biomedical Research, Department of Biology, Massachusetts Institute of Technology, Cambridge, Massachusetts 02142

Received May 28, 1998; Revised Manuscript Received July 23, 1998

ABSTRACT: Coiled coils consist of bundles of two or more α-helices that are aligned in a parallel or an antiparallel relative orientation. The designed peptides, Acid-p1 and Base-p1, associate in solution to form a parallel, heterodimeric two-stranded coiled coil [O'Shea, E. K., Lumb, K. J., and Kim, P. S. (1993) *Curr. Biol. 3*, 658]. The buried interface of this complex is formed by hydrophobic Leu residues, with the exception of an Asn residue from each strand that is positioned to engage in a buried polar interaction. Substitution of these buried Asn residues by Leu residues results in a loss of structural uniqueness, as evidenced by a lack of a particular helix orientation in the Acid−Base coiled-coil complex [Lumb, K. J., and Kim, P. S. (1995) *Biochemistry 34*, 8642]. Here, we alter the positions of the Asn residues in the Acid and Base peptides such that a buried polar interaction is only expected to occur when the helices are in an antiparallel orientation. The resulting peptides, Acid-a1 and Base-a1, associate to form a helical heterodimer, as shown by circular dichroism (CD) and equilibrium sedimentation centrifugation. The helix orientation preference has been measured using covalently linked, disulfide-containing heterodimers in which the constituent peptides are constrained to interact in either a parallel or an antiparallel orientation. Although both the parallel and antiparallel heterodimers form stable, helical structures, the antiparallel heterodimer is the predominant species at equilibrium when the heterodimers are allowed to undergo thiol−disulfide exchange. In addition, the antiparallel heterodimer is more stable to chemical denaturation than the parallel counterpart by approximately 2.3 kcal/mol. These results demonstrate that a single buried polar interaction in the interface between the helices of a coiled coil is sufficient to determine the relative orientation of its constituent helices.

The coiled coil, a widespread structural motif, is found in fibrous proteins, such as myosin and keratin (*1*), as well as in the bZip class of transcription factors, which contain coiled-coil dimerization domains (*2*−*4*). Coiled coils consist of two or more interacting α-helices, supercoiled around one another, that associate in a parallel or an antiparallel orientation. The α-helices of naturally occurring coiled coils are generally parallel. However, a growing number of proteins have been shown to contain antiparallel coiled-coil domains, including *Escherichia coli* and *Tetrahymena thermophilus* seryl tRNA synthetases, *E. coli* GreA, *Bacillus subtilis* replication terminator protein, *E. coli* AraC, and the ϵ-subunit of *E. coli* F_1-ATPase (*5*−*10*). Moreover, it has been shown that sequence features within a natural coiled coil can lead to a preference for an antiparallel helix orientation, rather than the more commonly observed parallel alignment (*11*).

The sequences of both parallel and antiparallel coiled coils are characterized by a heptad repeat of seven amino acid residues, denoted **a**−**g** (*12*). The residues at positions **a** and **d** are predominantly apolar, forming a 4−3 hydrophobic repeat, with charged residues occurring frequently at the **e** and **g** positions (*12*−*16*). Residues at these four positions participate in interhelical hydrophobic and electrostatic interactions (*4*, *17*−*19*).

"Peptide Velcro" is a designed, parallel, two-stranded, heterodimeric coiled coil formed by the peptides Acid-p1 and Base-p1 (*20*). These peptides have identical sequences at all but the **e** and **g** positions, at which Acid-p1 contains Glu residues whereas Base-p1 contains Lys residues. Thus, homodimers of both peptides are destabilized through electrostatic repulsion, leading to the formation of a heterodimer (*20*). Both peptides contain hydrophobic Leu residues at the interior **a** and **d** positions, with the exception of a polar Asn residue at position 14 of each peptide. This position was chosen by analogy with the GCN4 leucine zipper, in which Asn residues at comparable positions interact to form a hydrogen bond (*4*).

Although the burial of polar residues in the hydrophobic interior of a protein is destabilizing (*21*), buried polar residues are nonetheless a common feature of natural proteins (*22*, *23*). One explanation for the occurrence of buried polar residues is that they play a role in the specificity of protein folding. The importance of the Asn−Asn buried polar interaction in "Peptide Velcro" has been investigated (*24*). The Asn residues in the Acid-p1 and Base-p1 peptides were replaced by leucine. The Asn → Leu variants form a more stable complex that can no longer fold into a unique structure. Importantly, the helices lack a particular orientation. Thus,

† Supported by Grant GM44162 from the National Institutes of Health and a Helen Hay Whitney postdoctoral fellowship to M.G.O.

* To whom correspondence should be addressed.

‡ Present address: Department of Chemistry, Indiana University, Bloomington, IN 47405.

S0006-2960(98)01269-0 CCC: $15.00
Published on Web 08/19/1998

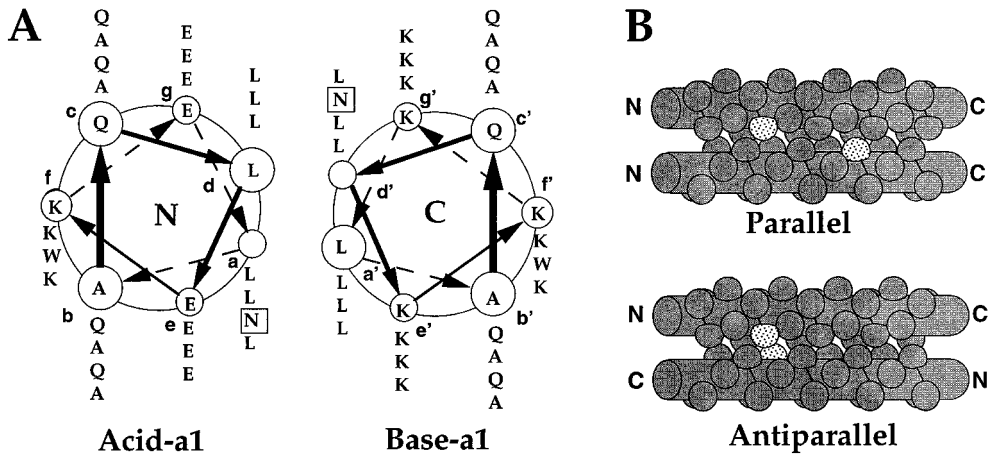

FIGURE 1: (A) Helical wheel representation of the antiparallel Acid-a1−Base-a1 heterodimer. The view is shown looking down the superhelical axis from the N terminus of Acid-a1 and the C terminus of Base-a1. The peptide sequence of Acid-a1 is Ac-AQLEKELQALEKELAQLE-WENQALEKELAQ-NH_2. The sequence for Base-a1 is Ac-AQLKKKLQANKKKLAQLKWKLQALKKKLAQ-NH_2. **(B)** Schematic view of parallel and antiparallel complexes of Acid-a1 and Base-a1, with the Asn residues represented by stippled semicircles. In the antiparallel complex, the two Asn residues can interact, but in the parallel complex, the Asn residues are separated by more than three turns of α-helix.

this buried polar interaction, though energetically unfavorable, imparts specificity for a parallel, two-stranded coiled coil (*24*).

To determine whether a buried polar interaction can impart specificity for other coiled-coil structures, we have changed the positions of the Asn residues in Acid-p1 and Base-p1 in "Peptide Velcro" such that they can interact only when the helices are in an antiparallel orientation. The resulting peptides, Acid-a1 and Base-a1 (Figure 1), associate to form a well-packed, heterodimeric complex with a pronounced preference for an antiparallel helix orientation. Thus, the positions of polar residues in the interface between the strands of a coiled coil can determine helix orientation in a model coiled coil.

MATERIALS AND METHODS

Peptide Preparation and Purification. Peptides Acid-a1, Acid-a1N, Acid-a1C, Base-a1, Base-a1N, and Base-a1C were synthesized by solid-phase methods and purified by reversed-phase HPLC,[1] using a Vydac C_{18} column and a linear water/acetonitrile gradient containing 0.1% trifluoroacetic acid as described previously (*20*). All peptides were acetylated at the N terminus and amidated at the C terminus. The identity of each peptide was confirmed by laser desorption mass spectrometry on a Voyager Elite mass spectrometer (PerSeptive Biosystems). In all cases, the observed and expected molecular masses agreed to within 0.1% of the calculated peptide mass. Disulfide-linked peptides were produced by air oxidation (0.1 M Na_2PO_4, pH 9.2) and purified by reversed-phase HPLC as previously described (*20*).

CD Spectroscopy. CD spectra were acquired with Aviv 60DS, Aviv 62DS, and Jasco J-715 spectropolarimeters. Samples were prepared in 10 mM sodium phosphate and 150 mM sodium chloride (PBS, pH 7.0) unless otherwise noted. Peptide concentrations were determined by Trp absorbance in 5−6 M GuHCl, assuming an extinction coefficient of 5600 M^{-1} cm^{-1} at 281 nm for Trp (*25*). The helix content was calculated by the method of Chen et al. (*26*). The wavelength dependence of $[\theta]$ was monitored at 25 °C in 1 nm increments with a sampling time of 10 s. The thermal stability was determined by monitoring the change in $[\theta]_{222}$ as a function of temperature. The temperature was increased in 2 °C increments with an equilibration time of 90 s and a data collection time of 30 s. All melts were reversible, provided that samples were not incubated at high temperatures for an extended period of time. Superimposable folding and unfolding curves were observed, and >90% of the signal was regained upon cooling.

Table 1: Molecular Weight Determination by Sedimentation Equilibrium Ultracentrifugation[a]

protein	concentration (μM)	M_r/M_r(calcd)
Acid-a1−Base-a1 (1:1)	100	0.98
	30	1.01
	10	0.97
Acid-a1C−Base-a1N	200	1.10
	100	1.08
	60	1.04
	20	1.03
	10	1.06
	5	1.01
Acid-a1N−Base-a1N	200	1.22[b]
	100	1.16[b]
	60	1.08
	20	1.05
	10	1.04
	5	0.99
Acid-a1N−Base-a1C	100	1.04
	30	1.04
	10	1.01
Acid-a1C−Base-a1C	100	1.04
	30	1.06
	10	1.03

[a] Initial concentrations for each sample are listed. [b] Nonrandom residuals in a plot of ln(absorbance) vs (radial distance)^2, fit assuming a model for a single ideal species.

[1] Abbreviations: $\Delta G°$, free energy of unfolding; $[\theta]_{222}$, molar ellipticity at 222 nm; k_{ex}, observed amide exchange rate; k_{int}, rate of amide exchange expected for an unfolded polypeptide; CD, circular dichroism; GuHCl, guanidine hydrochloride; HPLC, high-performance liquid chromatography; NEM, *N*-ethylmaleimide; NMR, nuclear magnetic resonance; T_m, midpoint of the thermal unfolding transition.

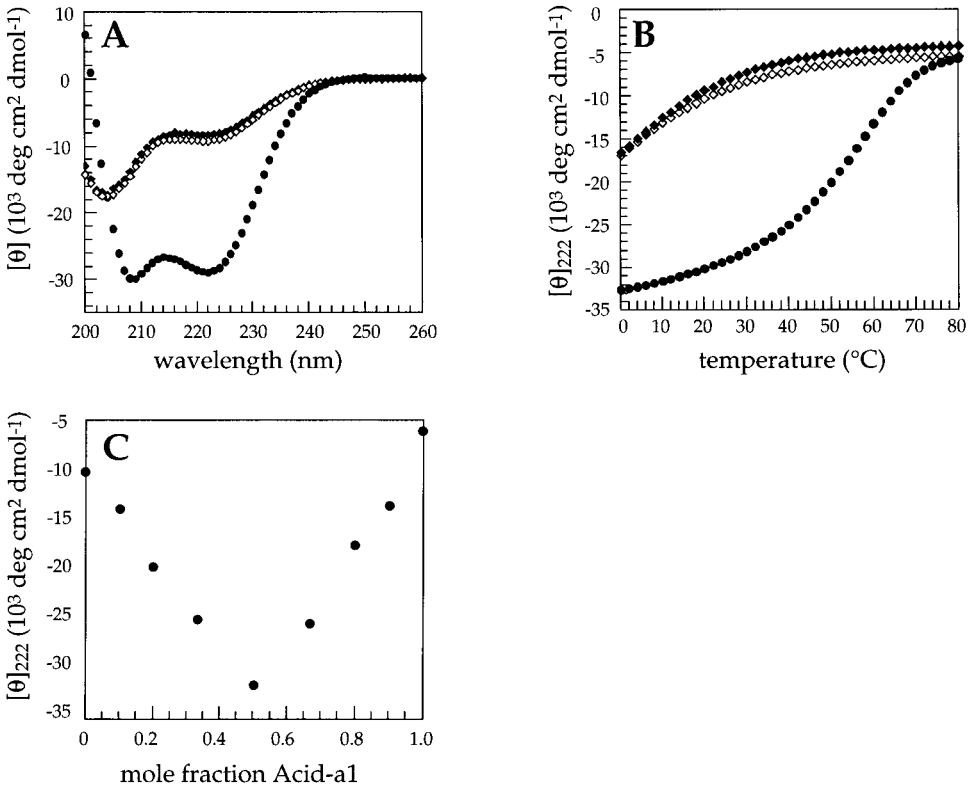

FIGURE 2: (A) Circular dichroism (CD) spectra of Acid-a1 (◆), Base-a1 (◇), and an equimolar mixture of Acid-a1 and Base-a1 (●). Spectra were recorded at 25 °C at a total peptide concentration of 20 μM in phosphate-buffered saline [PBS, 10 mM phosphate and 150 mM NaCl (pH 7)]. The minima at 210 and 222 nm for Acid-a1 and Base-a1 indicate that the equimolar mixture of peptides is highly helical. **(B)** Temperature dependence of the CD signal at 222 nm for the species described above (20 μM total peptide concentration, pH 7). Acid-a1 and Base-a1 are largely unfolded, but the equimolar mixture undergoes a cooperative thermal transition with a midpoint (T_m) of ~57 °C. (C) Dependence of the CD signal at 222 nm on the mole fraction of Acid-a1 at a constant total peptide concentration of 10 μM (25 °C, pH 7). The helicity of the mixture is maximal when Acid-a1 and Base-a1 are present in equimolar amounts, indicating that the stoichiometry of the peptides in the heterodimer is 1:1.

The stability to GuHCl denaturation was determined by monitoring $[\theta]_{222}$ as a function of GuHCl concentration at 25 °C in 10 mM sodium phosphate and 150 mM sodium chloride (pH 7.0). For comparison to NMR studies, the stability of Acid-a1N−Base-a1C to GuHCl denaturation was determined by monitoring $[\theta]_{222}$ as a function of deuterated GuHCl concentration at 25 °C in a D_2O buffer, containing 10 mM deuterated sodium phosphate and 150 mM sodium chloride (pH 6.0). Data were analyzed by the linear extrapolation method (*27*, *28*). pH readings in D_2O were not corrected for the isotope effect.

Sedimentation Equilibrium. Apparent molecular masses were determined by sedimentation equilibrium with a Beckman XL-A ultracentrifuge at 25 °C. Samples were dialyzed against 10 mM sodium phosphate and 150 mM sodium chloride (pH 7.0) for at least 6 h. Initial concentrations for each sample are listed in Table 1. Data obtained from two or three wavelengths at rotor speeds of 28 000 and 33 000 rpm were fit simultaneously to a single species model of ln(absorbance) versus (radial distance)^2 using the program NONLIN (courtesy of L. Johnson and J. Lary). Nonrandom residuals, indicative of aggregation or deviations from ideality, were observed only for Acid-a1N−Base-a1N at high concentrations (≥100 μM). Partial molar volumes and solvent densities were calculated as described by Laue et al. (*29*).

NMR Spectroscopy. NMR spectroscopy was performed with a Bruker AMX spectrometer operating at 500 MHz for ^1H. Samples were approximately 100 μM in 10 mM sodium phosphate and 150 mM sodium chloride (pH 6.0) and referenced internally to 0 ppm with trimethylsilylpropionic acid. One-dimensional data sets were acquired at 25 °C using a spectral width of 6024 Hz and solvent presaturation. Data sets were defined by 4096 complex points and zero-filled once before Fourier transformation. Hydrogen exchange studies were initiated by dissolving lyophilized samples in D_2O.

An average intrinsic amide exchange rate (k_{int}) of 11 min^{-1} was used, corresponding to 3 times the rate of amide exchange for poly-DL-alanine at pH 6.0 and 0 °C (*30*; see also the discussion in ref *24*). The overall exchange constants (k_{ex}) for the most highly protected amide resonances were estimated by an analysis of peak areas over eight time points between 1 and 28 h. The predicted protection factor (k_{int}/k_{ex}) expected for a global folding mechanism is equal to the reciprocal of the equilibrium constant for unfolding and was determined from the stability to guanidine denaturation as described above.

Disulfide Exchange. Helix orientation was determined using variants of the Acid-a1 and Base-a1 peptides with the following modifications. The sequence Cys-Gly-Gly was added to the N terminus of Acid-a1 to produce Acid-a1N; similarly, Gly-Gly-Cys was added to the C terminus of Acid-a1 to produce Acid-a1C. The sequences Trp-Cys-Gly-Gly and Gly-Gly-Cys-Trp were added at the N and C termini, respectively, of Base-a1 to generate the peptides Base-a1N

and Base-a1C. The two Gly residues provide flexibility for disulfide bond formation (*3*), and the additional Trp residue on the Base-a1 peptides facilitates HPLC separation of the heterodimers from the homodimers (*17*, *24*).

Peptides were incubated at room temperature (PBS, pH 7.0) in an anaerobic chamber to allow thiol−disulfide exchange. For qualitative determinations of helix orientation preference, equimolar amounts (10 μM) of Acid-a1N−Base-a1N and Acid-a1C, or of Acid-a1C−Base-a1N and Acid-a1N, were used. For quantitative determinations, the total ratio of Acid-a1C:Acid-a1N, including both free Acid-a1 species and the heterodimers, was held at 1:3. The reactions were quenched by addition of 1% NEM (9:1 water:acetonitrile) to a final concentration of 0.1%. After a 15 min reaction time, acetic acid was added (10% final concentration) and products were analyzed by reversed-phase HPLC on an analytical column (Vydac C_{18}) using a linear water/acetonitrile gradient containing 0.1% trifluoroacetic acid. Peptides were detected by absorbance at 229 nm. All peak assignments were verified by co-injection with an authentic standard. The extinction coefficients for the two heterodimers were assumed to be equal, as were those of Acid-a1C and Acid-a1N, on the basis of their identical amino acid content.

RESULTS

Acid-a1 and Base-a1 Form a Heterodimer. CD spectra (Figure 2A) demonstrate that the individual Acid-a1 and Base-a1 peptides are predominantly unfolded at 25 °C and pH 7 in phosphate-buffered saline (PBS). In contrast, the CD spectrum of an equimolar mixture of Acid-a1 and Base-a1 indicates that the mixture is highly helical (Figure 2A). This helical structure is also stable, exhibiting a cooperative thermal transition with a T_m of ∼57 °C at a total peptide concentration of 20 μM (Figure 2B). Sedimentation equilibrium studies of equimolar mixtures of Acid-a1 and Base-a1 show that these peptides form a dimer over a total peptide concentration range of 10−100 μM (Figure 3 and Table 1). Finally, the helical content monitored by $[\theta]_{222}$ of a mixture of Acid-a1 and Base-a1 is maximal when the two peptides are mixed in equimolar amounts (Figure 2C), indicating a stoichiometry of 1:1. Taken together, these data demonstrate that Acid-a1 and Base-a1 form a stable heterodimer in solution.

Helix Orientation. To probe the relative helix orientation in the Acid-a1−Base-a1 heterodimer, four additional peptides were synthesized: Acid-a1N, Acid-a1C, Base-a1N, and Base-a1C. The peptides denoted Acid-a1N and Base-a1N contain an N-terminal Cys-Gly-Gly sequence, and a Gly-Gly-Cys sequence is appended to Acid-a1C and Base-a1C at their C termini. Covalently linked heterodimers, constrained to interact in either a parallel or an antiparallel orientation, were produced through oxidation of the appropriate Cys-containing peptides (*3*). CD studies show that both the antiparallel, covalently linked heterodimer, Acid-a1C−Base-a1N, and its parallel counterpart, Acid-a1N−Base-a1N (Figure 4A), are highly helical at 25 °C.

Sedimentation equilibrium experiments (Table 1) indicate that the Acid-a1N−Base-a1N heterodimer does not aggregate at concentrations used in CD experiments (10 μM). Thus, the observation that the parallel Acid-a1N−Base-a1N heterodimer adopts a helical conformation suggests that isolated Asn residues can be accommodated at a hydrophobic interface position of a coiled coil. As it is not clear how this isolated polar residue can be accommodated at a buried position, it would be interesting to determine the structure of a heterodimer such as Acid-a1N−Base-a1N.

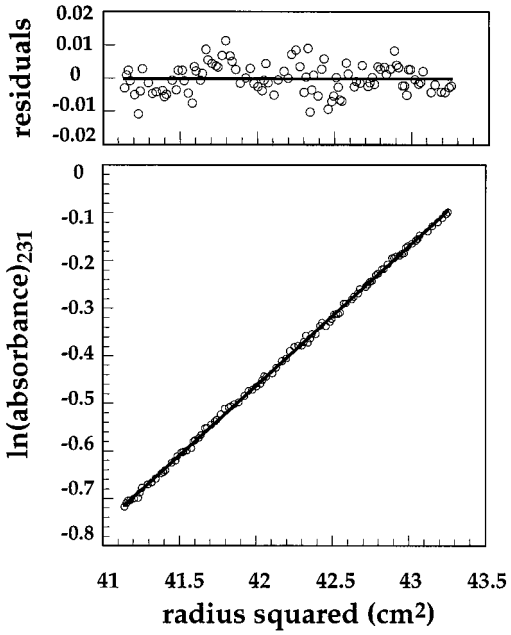

FIGURE 3: Representative analytical ultracentrifugation data for Acid-a1−Base-a1 at a single wavelength (25 °C, 30 μM, and pH 7.0). Data were collected at two rotor speeds (28 000 and 33 000 rpm) and two or three wavelengths for three initial peptide concentrations ranging from 10 to 100 μM. The apparent molecular weight did not vary across this range (Table 1). A random distribution of residuals indicates that the data fit well to an ideal single-species model. The observed molecular weight was 7180 and that calculated for the heterodimer 7122.

Nonetheless, the antiparallel Acid-a1C−Base-a1N heterodimer is substantially more stable to thermal denaturation than the parallel heterodimer (Figure 4B). Similar results were obtained with Acid-a1N−Base-a1C and Acid-a1C−Base-a1C (data not shown), suggesting that the helicity and stability of the heterodimers are independent of the disulfide linker position. Thus, the heterodimer formed by the Acid-a1 and Base-a1 peptides has a substantial preference for an antiparallel alignment of its constituent helices.

Measuring Orientation Preference. The preference for an antiparallel helix orientation was monitored using an equilibrium thiol−disulfide exchange assay (Figure 5A) (*17*, *24*). Equimolar amounts (10 μM, pH 7) of Acid-a1N−Base-a1N and Acid-a1C were mixed in an inert atmosphere and allowed to equilibrate (Figure 5B). The observed equilibrium should reflect the relative stabilities of the parallel and antiparallel disulfide-linked heterodimers. The predominant species observed are Acid-a1C−Base-a1N and Acid-a1N, demonstrating that the antiparallel relative helix orientation is preferred under equilibrium conditions. When equimolar amounts of Acid-a1N and Acid-a1C−Base-a1N (10 μM, pH 7) are mixed (Figure 5C), the observed product ratios are equivalent to those observed when the rearrangement proceeds from the parallel heterodimer, confirming that the reaction mixtures have reached equilibrium.

The observed apparent equilibrium constant in the disulfide rearrangement assay, however, was found to be dependent

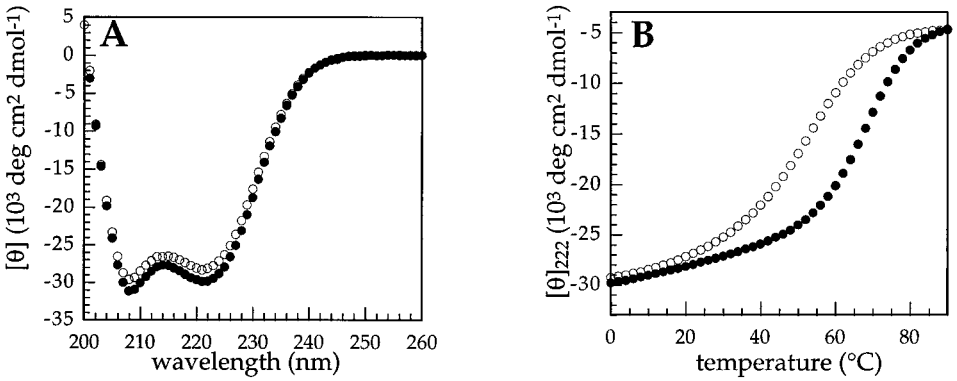

FIGURE 4: (A) CD spectra for Acid-a1N−Base-a1N (○; pH 7, 25 °C, and 10 μM peptide) and Acid-a1C−Base-a1N (●; PBS, pH 7, 25 °C, and 10 μM peptide). The minima at 210 and 222 nm indicate that both species are highly helical under these conditions. **(B)** Temperature dependence of the CD signal at 222 nm for the species described above (10 μM peptide, pH 7, and 1.5 M GuHCl). Guanidine hydrochloride is included to destabilize the complexes such that the thermal transition is complete at 90 °C. The T_m of the thermal unfolding transition is ~68 °C for Acid-a1C−Base-a1N; the T_m of the thermal unfolding transition is ~52 °C for Acid-a1N−Base-a1N.

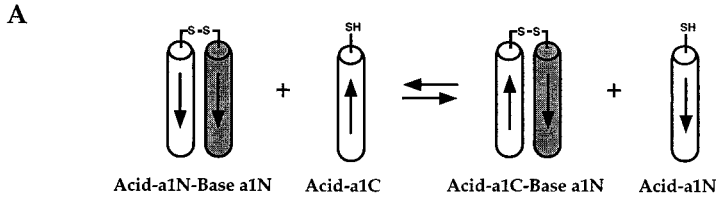

$$K_{eq} = \frac{[\text{Acid-a1C-Base-a1N}]\,[\text{Acid-a1N}]}{[\text{Acid-a1N-Base-a1N}]\,[\text{Acid-a1C}]}$$

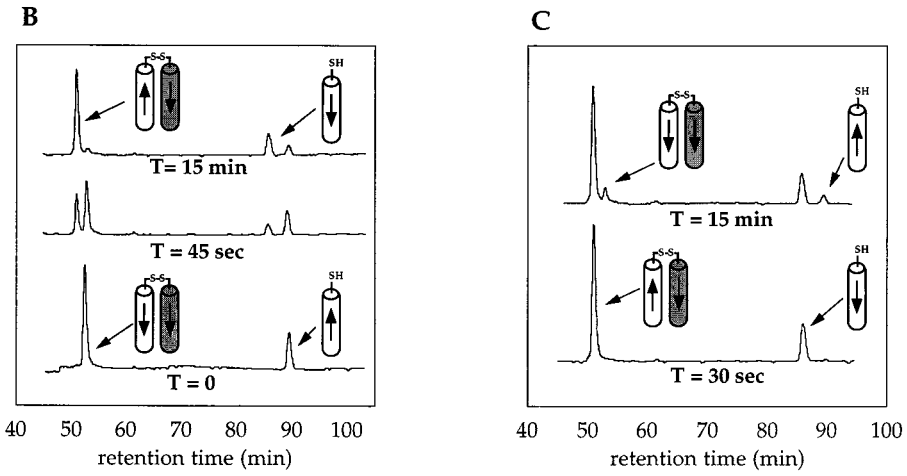

FIGURE 5: (A) Schematic view of the equilibrium thiol−disulfide exchange assay. Acid-a1 species are shown in white. Base-a1 species are shaded. Arrows indicate the direction of the peptide chain from the N to the C terminus. All rearrangements were carried out in PBS buffer (pH 7) at approximately 23 °C. Reactions were allowed to proceed for the indicated time, and then NEM was added to a final concentration of 0.1% to quench the reactions (see Materials and Methods). **(B)** HPLC chromatogram showing the progress of the rearrangement from Acid-a1C (10 μM) and Acid-a1N−Base-a1N (10 μM) to a solution in which the predominant species are Acid-a1C−Base-a1N and Acid-a1N. **(C)** HPLC chromatogram showing the progress of the rearrangement from Acid-a1N (10 μM) and Acid-a1C−Base-a1N (10 μM).

on the total peptide concentration. To obtain roughly equal peak areas for accurate quantitation, the equilibrium was driven toward the parallel species by the inclusion of an additional 2 equiv of Acid-a1N in the rearrangement assays. Thus, a 1:2:1 ratio of Acid-a1N−Base-a1N:Acid-a1N:Acid-a1C was used for rearrangements from the parallel heterodimer, and a 1:3 ratio of Acid-a1C−Base-a1N:Acid-a1N was used for rearrangements from the antiparallel heterodimer. As the total peptide concentration is increased, over a range of initial heterodimer concentrations of 1−50 μM, the apparent preference for an antiparallel helix orientation decreases. The inherent preference for a parallel or antiparallel relative helix alignment is not expected to be concentration-dependent, suggesting that higher-order species are formed. Nonetheless, sedimentation equilibrium experiments demonstrate that the heterodimers do not form higher-order species in this concentration range (Table 1). Thus, the most likely explanation for the concentration dependence of the apparent equilibrium constant is that the additional equivalents of Acid-a1 associate with the heterodimers to form higher-order species that distort our measurements of relative helix orientation for the Acid-a1 and Base-a1

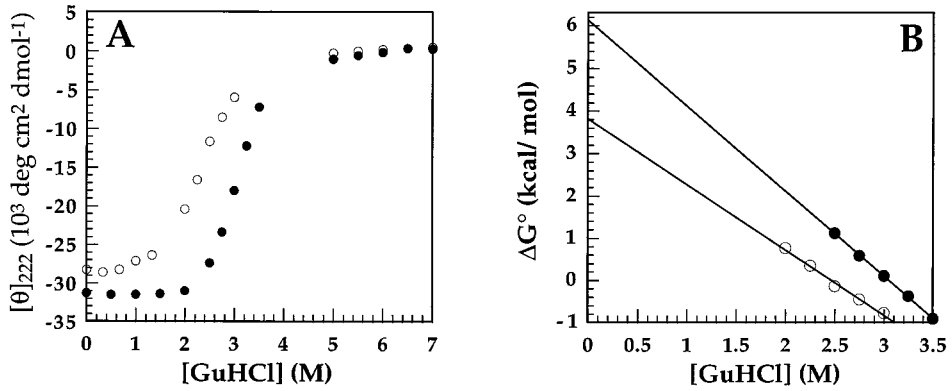

FIGURE 6: (A) GuHCl denaturation curves for Acid-a1C−Base-a1N (●; 25 °C, 10 μM peptide, and pH 7) and Acid-a1N−Base-a1N (○; 25 °C, 11 μM peptide, and pH 7). **(B)** The data yield apparent $\Delta G°$ values of -6.1 ± 0.2 and -3.8 ± 0.5 kcal/mol for Acid-a1C−Base-a1N (●) and Acid-a1N−Base-a1N (○), respectively.

peptides. At lower peptide concentrations, the extent of formation of higher-order species is reduced, and the observed apparent equilibrium constant more accurately reflects the inherent antiparallel preference. Although the apparent equilibrium values do not converge to a true equilibrium constant in the range of concentrations in which they could be accurately measured in this assay, the measurements at 1 μM peptide indicate a preference for the antiparallel helix orientation by a factor of ~40:1, which we conclude is a measure of the lower limit for the actual preference.

An independent measurement of the magnitude of the antiparallel helix orientation preference was made by determining the stability to chemical denaturation of both the antiparallel and parallel disulfide-linked heterodimers, Acid-a1C−Base-a1N and Acid-a1N−Base-a1N, respectively (Figure 6). From the difference in the stability of these two species, the magnitude of the helix orientation preference can be calculated. The measured stability of Acid-a1C−Base-a1N is 2.3 kcal/mol higher than that of Acid-a1N−Base-a1N (Figure 6), suggesting that the Acid-a1 and Base-a1 peptides prefer an antiparallel helix orientation by a factor of ~50:1.

Hydrogen Exchange Studies. In contrast to many designed proteins, naturally occurring globular proteins typically contain a subset of amide protons with hydrogen exchange rates approximately 1 order of magnitude slower than expected if exchange occurs only from globally unfolded molecules (see ref *24* and references therein). Hydrogen exchange studies can therefore be used as a measure of the degree to which designed proteins contain a well-packed, native-like interior. The most slowly exchanging amide protons in "Peptide Velcro" have exchange rates consistent with a global unfolding exchange mechanism, suggesting a well-packed interior (*20*, *24*). In contrast, the most slowly exchanging amide protons in an equimolar mixture of the Asn → Leu variants of Acid-p1 and Base-p1 exchange 2 orders of magnitude more quickly than would be expected for a global unfolding mechanism, suggesting that this protein has a fluctuating structure (*24*).

Hydrogen exchange studies of an equimolar mixture of Acid-a1 and Base-a1 (1 mM total peptide concentration, pH 7.0, and 20 °C) reveal no strongly protected amide protons under these conditions (data not shown). Because the helix orientation is not absolute, the Acid-a1 and Base-a1 peptides are expected to exist as a mixture of the predominant species, the antiparallel heterodimer, and a minor parallel component. Thus, it is possible that rapid hydrogen exchange occurs not through the antiparallel heterodimer, but through the parallel species, or during the interconversion between the parallel and antiparallel species present in an equimolar mixture of Acid-a1 and Base-a1.

The hydrogen exchange properties of the disulfide-linked antiparallel heterodimer, Acid-a1C−Base-a1N, were therefore investigated. A small subset of amide protons in Acid-a1C−Base-a1N is strongly protected from amide exchange (Figure 7B; 100 μM peptide, pH 6.0, and 25 °C). The most protected amide protons exchange more slowly than expected from the global stability of the heterodimer, as determined by GuHCl denaturation in D_2O (Figure 7A). Thus, the Acid-a1−Base-a1 helical interface is well-packed.

DISCUSSION

The interaction between buried polar Asn residues in "Peptide Velcro", though energetically unfavorable, imparts specificity for a parallel, two-stranded structure (*20*, *24*). Substitution of Leu for the interior Asn residues results in a heterotetramer in which the helices lack a particular orientation, suggesting that helix orientation can be determined by a single interaction. Antiparallel, two-stranded coiled coils are much less common than their parallel counterparts. In addition, the isolated constituent helices of the two-stranded, antiparallel coiled coil from *E. coli* seryl tRNA synthetase fail to associate stably in the absence of a covalent tether (*11*). Thus, the requirements for the design of an antiparallel, two-stranded coiled coil are less well understood than those for parallel coiled coils, and such a structure may be more difficult to stabilize.

When the positions of the Asn residues in the Acid−Base coiled coil are changed such that they can interact only if the constituent helices are in an antiparallel orientation, the predominant species is an antiparallel coiled coil. Significantly, Acid-a1 and Base-a1 associate to form a stable, two-stranded structure with a strong antiparallel preference in the absence of a covalent tether, in contrast to other designed antiparallel coiled coils (*31*−*37*). A single buried polar interaction can therefore specify either a parallel or an antiparallel helix orientation in a two-stranded coiled coil.

Buried polar interactions have also been shown to be important in determining specificity for homo- or het-

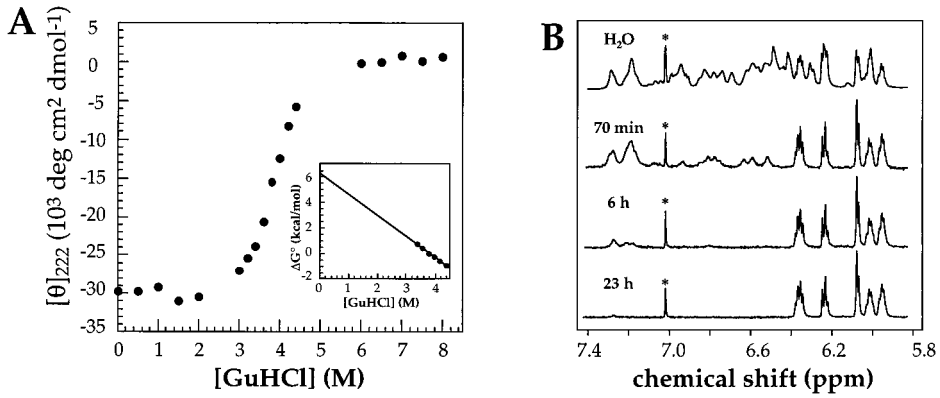

FIGURE 7: (A) GuHCl denaturation curve for Acid-a1C−Base-a1N (25 °C, 20 μM peptide, pH 6, and D_2O). The data yield an apparent $\Delta G°$ of -6.3 ± 0.6 kcal/mol (inset). **(B)** ^{1}H amide hydrogen exchange studies of Acid-a1C−Base-a1N (25 °C, pH 6.0, and ca. 100 μM protein). A total of 16 384 scans were used to collect the data in water, and 4096 or 8192 scans were used to collect the data in D_2O. The resonance marked by an asterisk arises from an impurity. The predicted protection factor (k_{int}/k_{ex}) expected from the global stability of the molecule is 10^4; the observed protection factor for the most slowly exchanging amides is 10^4-10^5. These results provide strong evidence that Acid-a1C−Base-a1N has a well-packed interior (see the text).

erodimerization in parallel coiled coils. For instance, genetic screens have been used to isolate variants of the bZip proteins Jun, Fos, C/EBP, and GCN4 with altered dimerization specificity determined by the positioning of asparagine residues at interior **a** positions (*38*). In addition, variants of GCN4, in which Asn residues at **a** positions are replaced with Asp and 2,4-diaminobutyric acid residues, preferentially form heterodimers (*39*).

A single hydrogen bond is formed between Asn residues at the **a** and **a′** positions in the interior of GCN4 (*4*). Our results indicate that the analogous **a**−**d′** interaction (Figure 1) can be used to stabilize an antiparallel coiled coil. However, such interactions have not been observed in naturally occurring coiled coils. Instead, an interaction has been observed in the seryl tRNA synthetase coiled coil between Arg-54 at a **d** position on one strand and Glu-74 at a **g′** position in the other (*5*). A similar **a**−**e′** interaction is seen in the GreA coiled coil (*7*). As the analogous **a**−**g′** interaction has also been observed in parallel coiled coils (*19*), this type of buried polar interaction may also play a role in orientation specificity.

Other differences between parallel and antiparallel coiled coils have been proposed to contribute to helix orientation specificity. For instance, it has been suggested that the relative position of large and small hydrophobic residues in the interior of a coiled coil influences helix orientation preference (*34*, *40*). In addition, the presence of potentially attractive or repulsive interactions at the **e** and **g** positions has been reported to affect orientation preference in model coiled coils (*32*, *33*).

In Acid-a1, Glu residues are found at both the **e** and **g** positions, while these positions in Base-a1 are occupied by Lys residues. The potential electrostatic interactions are therefore similar in both the parallel and antiparallel orientations and are not expected to contribute to the observed antiparallel specificity. Similarly, apart from the single Asn residue in each peptide, the interior residues are Leu, ruling out complementary size interactions in determining antiparallel specificity. Remarkably, the potential for a buried polar interaction between Asn residues at the **a** and **d′** positions of Acid-a1 and Base-a1, respectively, is sufficient to specify an antiparallel helix orientation in the absence of other interactions expected to favor an antiparallel coiled coil. The positions of Asn residues in the interior of a coiled coil can therefore be used to position the helices in an antiparallel orientation, and the incorporation of additional interactions would be expected to enhance the observed antiparallel specificity.

ACKNOWLEDGMENT

We thank M. W. Burgess and J. Pang for peptide synthesis and mass spectrometry, L. Huff for assistance with peptide purification, K. J. Lumb for assistance with NMR experiments, D. Fass and J. J. Hollenbeck for careful reading of the manuscript, and K. J. Lumb, P. B. Harbury, and L. C. Wu for many helpful discussions.

REFERENCES

1. Cohen, C., and Parry, D. A. D. (1990) *Proteins 7*, 1.
2. Landschulz, W. H., Johnson, P. F., and McKnight, S. L. (1988) *Science 240*, 1759.
3. O'Shea, E. K., Rutkowski, R., and Kim, P. S. (1989) *Science 243*, 538.
4. O'Shea, E. K., Klemm, J. D., Kim, P. S., and Alber, T. A. (1991) *Science 254*, 539.
5. Cusack, S., Berthet-Colominas, C., Hartlein, M., Nassar, N., and Leberman, R. (1990) *Nature 347*, 249.
6. Biou, V., Yaremchuk, A., Tukalo, M., and Cusack, S. (1994) *Science 263*, 1404.
7. Stebbins, C. E., Borukhov, S., Orlova, M., Polyakov, A., Goldfarb, A., and Darst, S. A. (1995) *Nature 373*, 636.
8. Bussiere, D. E., Bastia, D., and White, S. W. (1995) *Cell 80*, 651.
9. Soisson, S. M., MacDougall-Shackleton, B., Schleif, R., and Wolberger, C. (1997) *Science 276*, 421.
10. Uhlin, U., Cox, G. B., and Guss, J. M. (1997) *Structure 5*, 1219.
11. Oakley, M. G., and Kim, P. S. (1997) *Biochemistry 36*, 2544.
12. McLachlan, A. D., and Stewart, M. (1975) *J. Mol. Biol. 98*, 293.
13. Hodges, R. S., Sodek, J., Smillie, L. B., and Jurasek, L. (1972) *Cold Spring Harbor Symp. Quant. Biol. 37*, 299.
14. Parry, D. A. D. (1982) *Biosci. Rep. 2*, 1017.
15. Lupas, A., Van Dyke, M., and Stock, J. (1991) *Science 252*, 1162.
16. Berger, B., Wilson, D. B., Tonchev, T., Milla, M., and Kim, P. S. (1995) *Proc. Natl. Acad. Sci. U.S.A. 92*, 8259.
17. Harbury, P. B., Zhang, T., Kim, P. S., and Alber, T. (1993) *Science 262*, 1401.
18. Harbury, P. B., Kim, P. S., and Alber, T. (1994) *Nature 371*, 80.

19. Glover, J. N. M., and Harrison, S. C. (1995) *Nature 373*, 257.
20. O'Shea, E. K., Lumb, K. J., and Kim, P. S. (1993) *Curr. Biol. 3*, 658.
21. Sauer, R. T., and Lim, W. A. (1992) *Curr. Opin. Struct. Biol. 2*, 46.
22. Barlow, D. J., and Thornton, J. M. (1983) *J. Mol. Biol. 168*, 867.
23. Rashin, A. A., and Honig, B. (1984) *J. Mol. Biol. 173*, 515.
24. Lumb, K. J., and Kim, P. S. (1995) *Biochemistry 34*, 8642.
25. Edelhoch, H. (1967) *Biochemistry 6*, 1948.
26. Chen, Y., Yang, J. T., and Chau, K. H. (1974) *Biochemistry 13*, 3350.
27. Tanford, C. (1970) *Adv. Protein Chem. 24*, 1.
28. Pace, C. N. (1986) *Methods Enzymol. 131*, 266.
29. Laue, T. M., Shah, B. D., Ridgeway, T. M., and Pelletier, S. L. (1992) in *Analytical Ultracentrifugation in Biochemistry and Polymer Science* (Harding, S. E., Rowe, A. J., and Horton, H. C., Eds.) p 90, The Royal Society of Chemistry, Cambridge, England.
30. Englander, S. W., Downer, N. W., and Teitelbaum, H. (1972) *Annu. Rev. Biochem. 41*, 903.
31. Lombardi, A., Bryson, J. W., Ghirlanda, G., and DeGrado, W. F. (1997) *J. Am. Chem. Soc. 119*, 12378.
32. Monera, O. D., Zhou, N. E., Kay, C. M., and Hodges, R. S. (1993) *J. Biol. Chem. 268*, 19218.
33. Monera, O. D., Kay, C. M., and Hodges, R. S. (1994) *Biochemistry 33*, 3862.
34. Monera, O. D., Zhou, N. E., Lavigne, P., Kay, C. M., and Hodges, R. S. (1996) *J. Biol. Chem. 271*, 3995.
35. Monera, O. D., Zhou, N. E., Sönnichsen, F. D., Hicks, L., Kay, C. M., and Hodges, R. S. (1996) *Protein Eng. 9*, 353.
36. Kuroda, Y., Nakai, T., and Ohkubo, T. (1994) *J. Mol. Biol. 236*, 862.
37. Myszka, D. G., and Chaiken, I. M. (1994) *Biochemistry 33*, 2363.
38. Zeng, X., Herndon, A. M., and Hu, J. C. (1997) *Proc. Natl. Acad. Sci. U.S.A. 94*, 3673.
39. Schneider, J. P., Lear, J. D., and DeGrado, W. F. (1997) *J. Am. Chem. Soc. 119*, 5742.
40. Gernert, K. M., Surles, M. C., Labean, T. H., Richardson, J. S., and Richardson, D. C. (1995) *Protein Sci. 4*, 2252.

BI981269M